DeMay et al., http://www.jcb.org/cgi/content/full/jcb.201012143/DC1

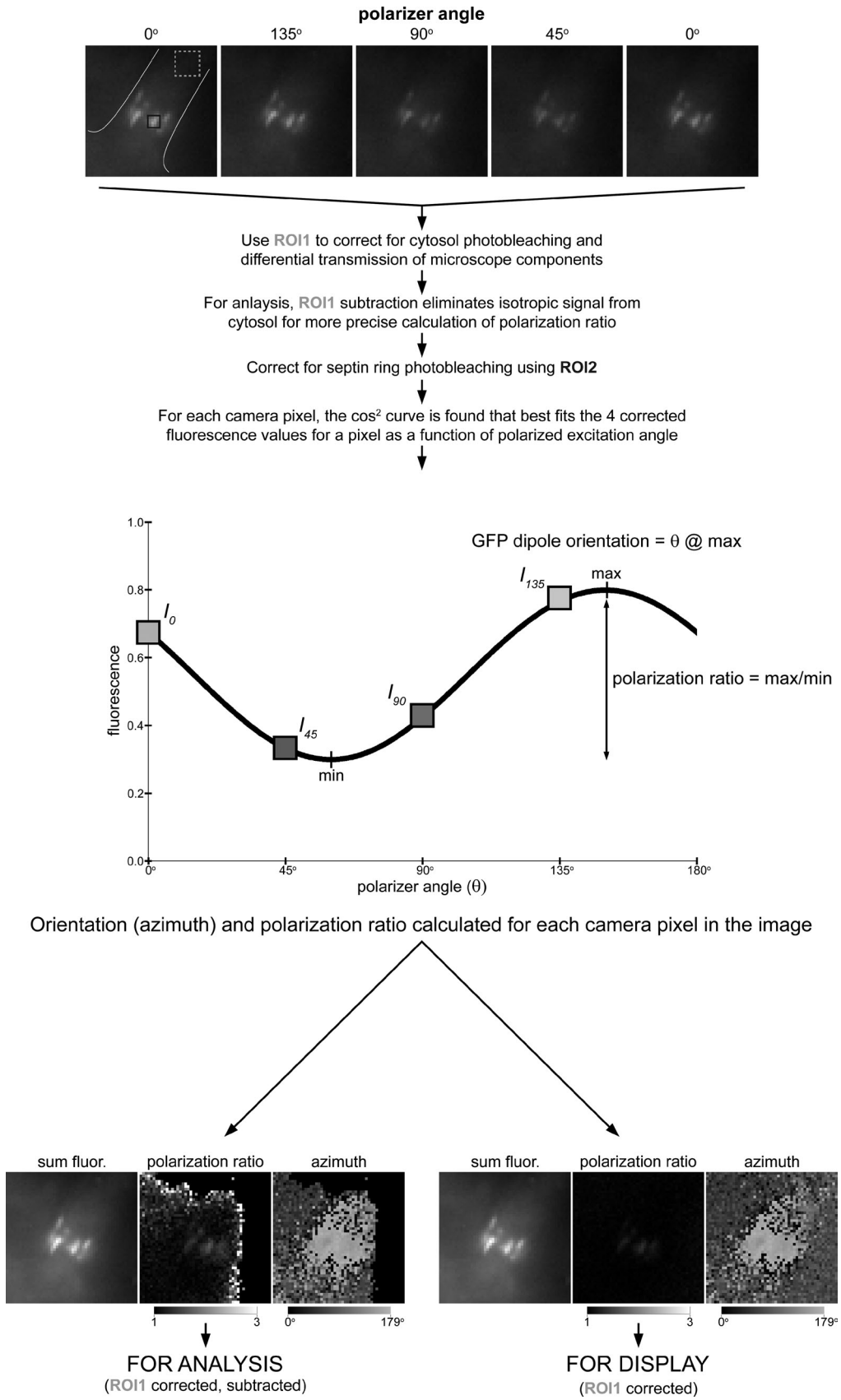


Figure S1. **Calculation of polarization ratio and dipole orientation.** Summary of the analysis of fluorescence images that was performed using software developed for these studies and an overview of the preparation of images for use in quantitative analysis and display. The raw data (top image sequence) was corrected for background fluorescence, cytosolic photobleaching, septin-fluorescence photobleaching, and differential transmission of light caused by microscope optics using the regions of interest (ROIs) noted on the images. For each pixel across the corrected images, the $\cos^2$ curve is found that provides the best fit as a function of polarizer angle. The polarizer angle corresponding to the maximum amplitude of this fit curve is the mean GFP dipole orientation (azimuth), whereas the polarization ratio is the ratio of the maximum and minimum values of the curve. If background fluorescence is not subtracted out, the polarization ratio will necessarily decrease. Therefore, all data prepared for quantitative analysis was background corrected. This background fluorescence correction was not applied to images for display as it creates artificially high polarization ratios in areas where there is very little real fluorescence (seen in the polarization ratio of the bottom-left images sequence).

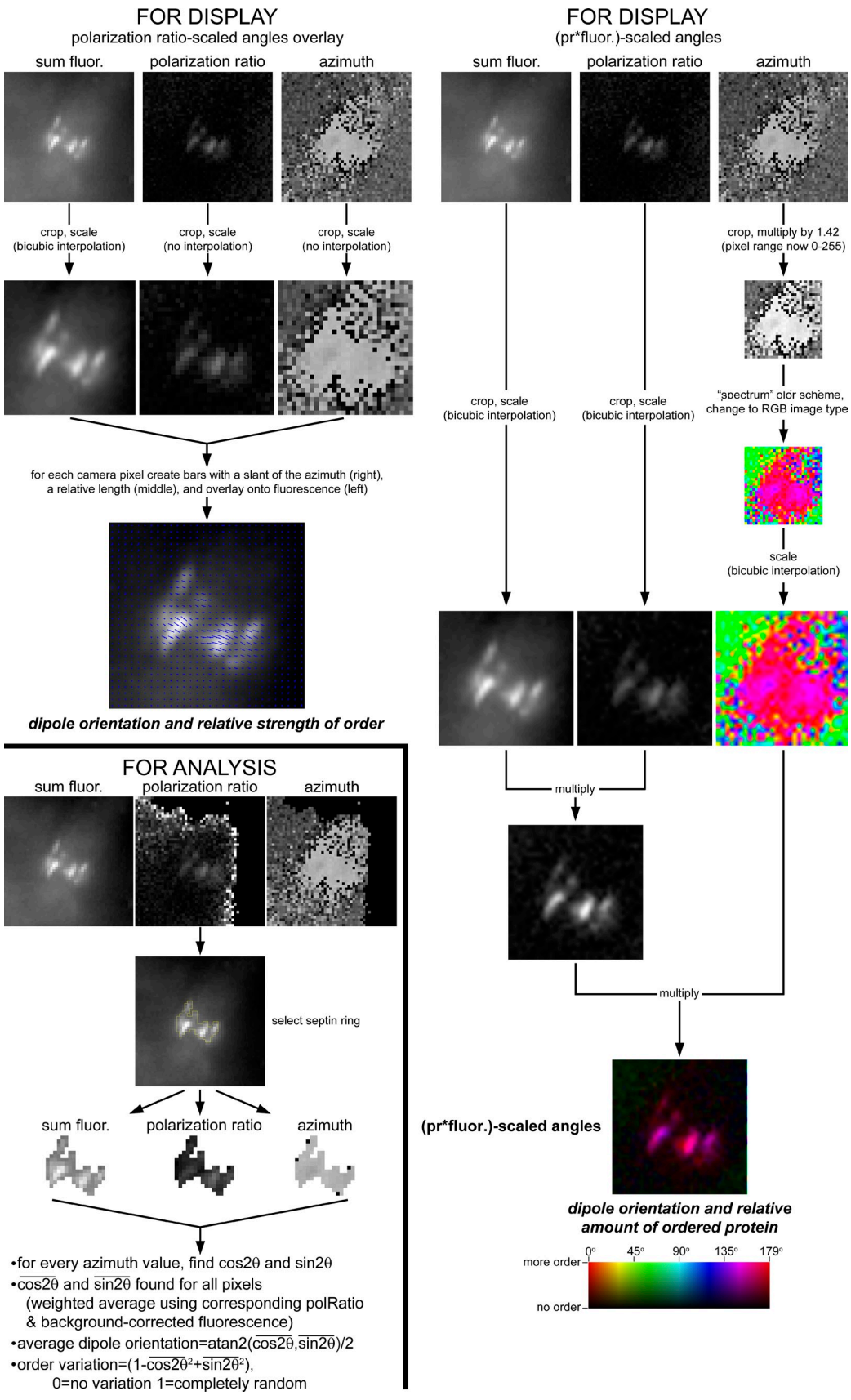


Figure S2. **Image processing for display and quantitative analysis of septin rings. A** graphical step-by-step review of methods used to create the blue line overlay and scaled color images. The blue lines were created using a custom ImageJ plugin developed for these studies. For a given pixel, a blue line can be created with an orientation of that pixel coordinate's value in the azimuth map and scaled in length according to its value in the polarization ratio map. To create the (pr*fluor.)-scaled color images, the azimuth map is multiplied by 1.42 to increase the range of pixel values from 0–179 to 0–255. The image is then displayed using the "spectrum" color scheme available in ImageJ and subsequently changed to an RGB image type. This color image is then scaled in intensity by the product of the sum fluorescence image and the polarization ratio map, and linearly contrast enhanced. Bottom left, a graphical step-by-step review of methods used to calculate mean dipole angles for a septin structure.

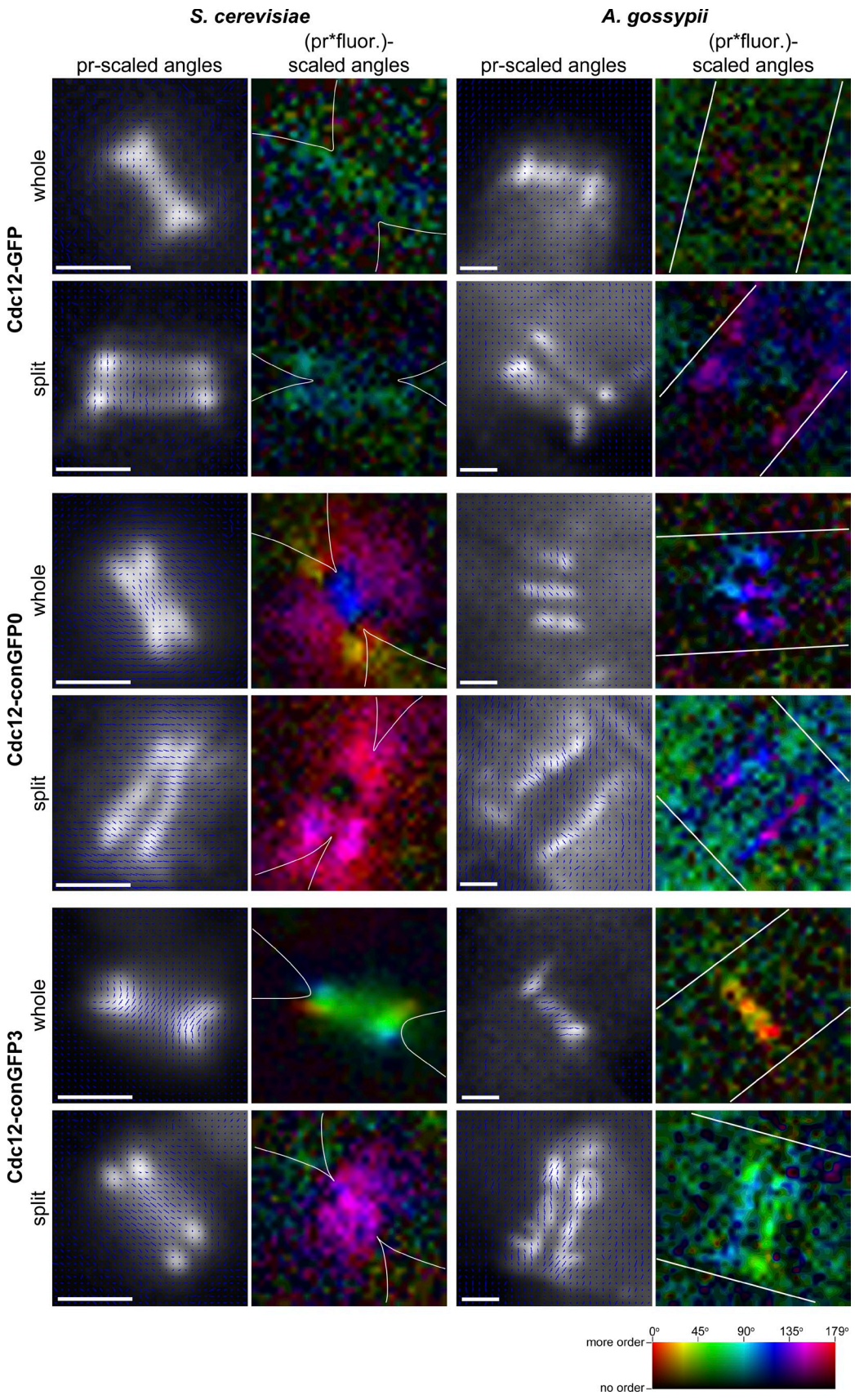


Figure S3. **Additional constructs show ordered organization in septin rings in *A. gossypii* and *S. cerevisiae*.** Whole and split septin rings assembled in *A. gossypii* or *S. cerevisiae* cells expressing the noted septin-conGFP construct from a plasmid. Cell outlines are shown in white. Bars, 1 µm.

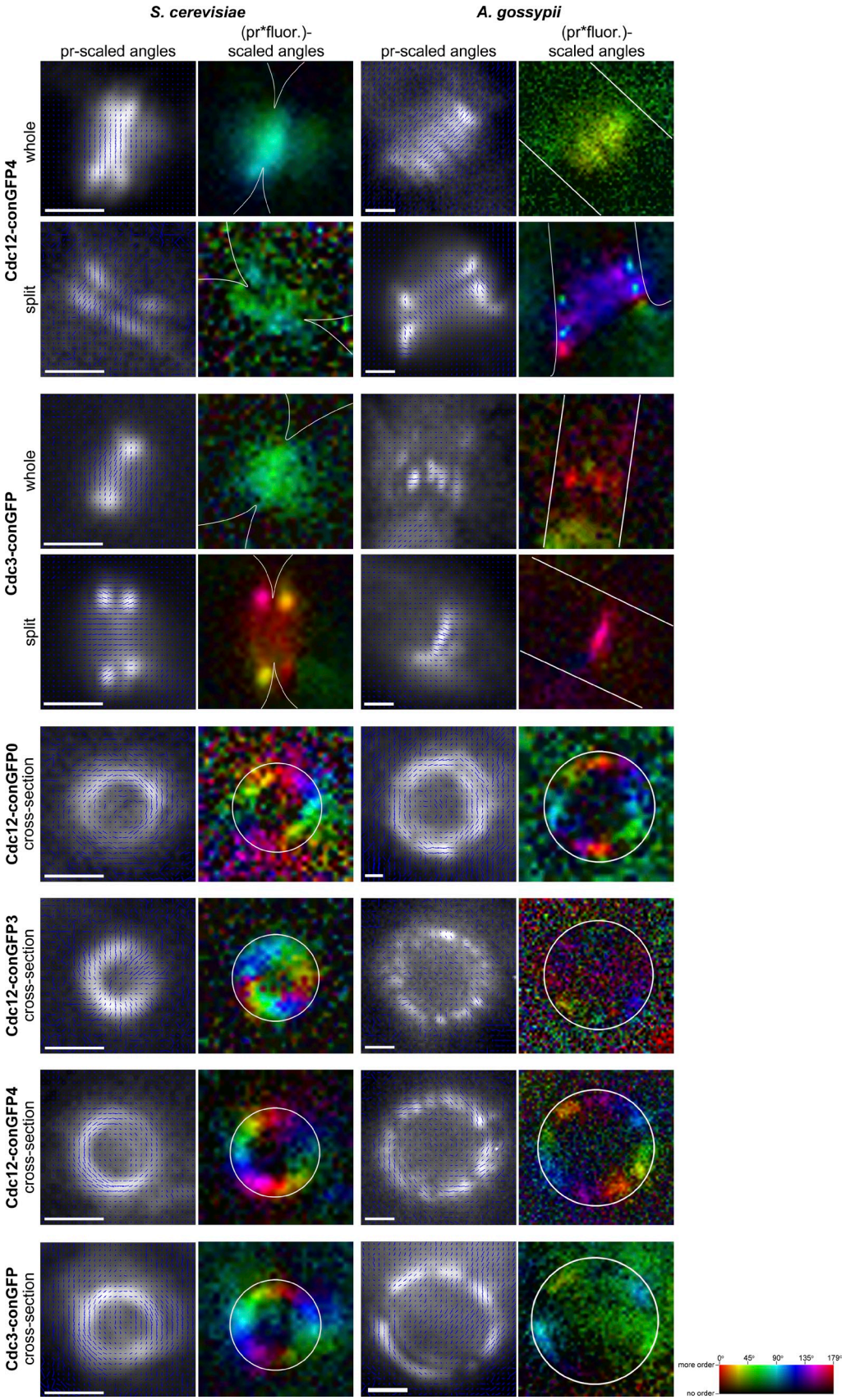


Figure S4. **Additional constructs show ordered organization in septin rings in *A. gossypii* and *S. cerevisiae*.** Whole and split septin rings assembled in *A. gossypii* or *S. cerevisiae* cells expressing the noted septin-conGFP construct from a plasmid. The lower half of the image panels are septin rings viewed from the xz (cross-section) perspective. Cell outlines are shown in white. Bars, 1 μm.

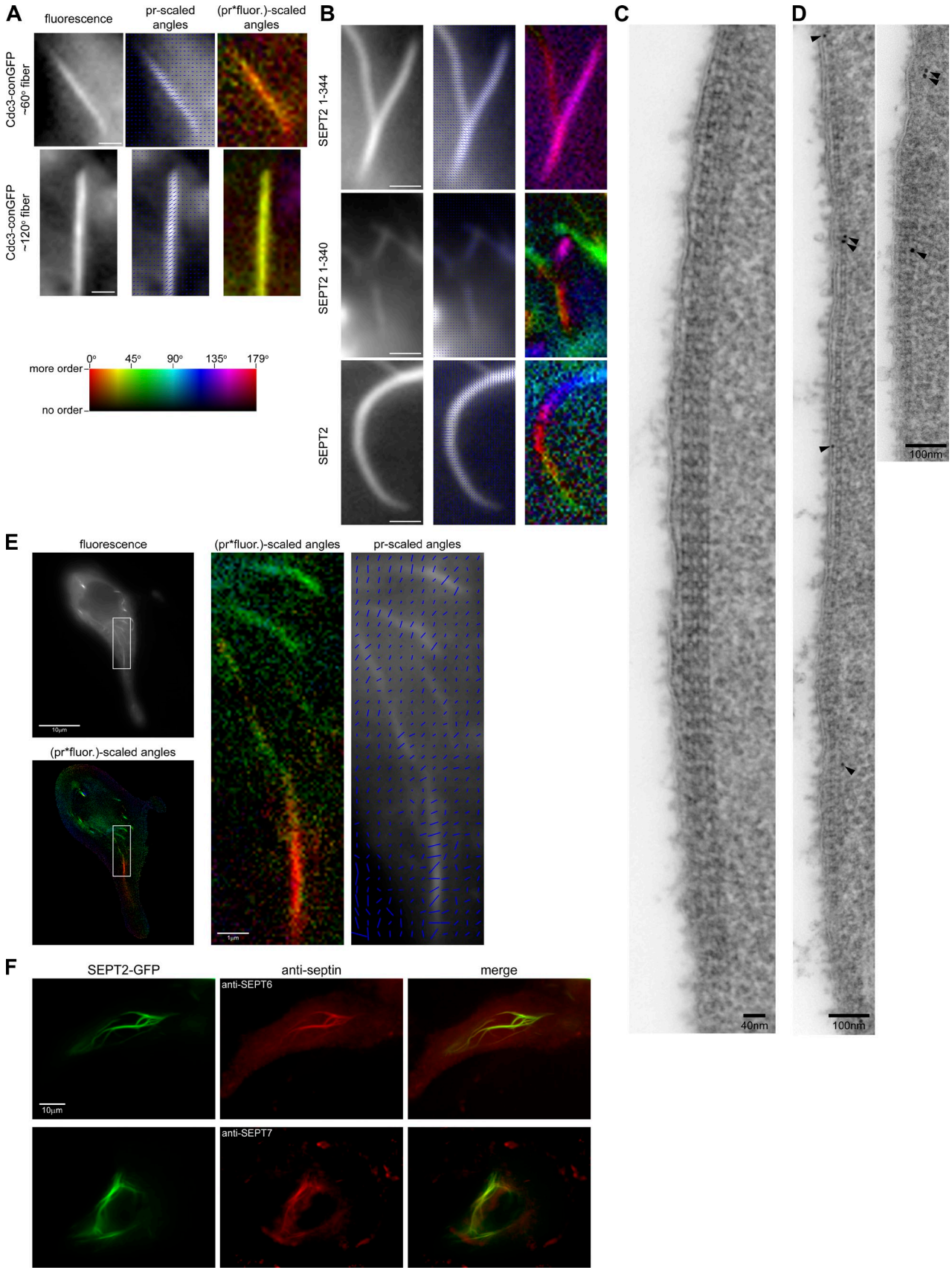


Figure S5. **Additional examples of septin fibers.** (A) Septin fibers formed in *A. gossypii* cells expressing Cdc3-conGFP. (B) Septin fibers formed in MDCK cells expressing various SEPT2 fusion constructs. (C) TEM of septin fibers at the cell cortex in *A. gossypii* showing stacked or bundled septin filaments. (D) TEM of *SHS1-6HA* expressing cells with an immunolabeled section (AG296), in which septins have been localized using an anti-HA primary and a 10-nm gold–conjugated secondary antibody. The entire paired filament immunolabeled shown in Fig. 3 is displayed here, with seven gold particles visible. Arrowheads point to gold particles. (E) An MDCK cell expressing SEPT2–conGFP-1-344 at a lower level than shown in Fig. 5. Consistent with Fig. 5, the azimuth of the measured fluorescence anisotropy is oriented perpendicular to the fiber axis. The white frames identify the magnified regions shown on the right. (F) MDCK cells expressing SEPT2–conGFP-1-344 were fixed and processed for immunofluorescence against SEPT6 or SEPT7. Merged image panels highlight the colocalization of these antibodies with the fusion protein. Bars: (A and B) 1 µm; (E, left) 10 µm; (E, right) 1 µm; (F) 10 µm.

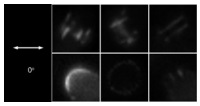

Video 1. **Polarized fluorescence acquisition of *A. gossypii* septin rings.** The "video" consists of 4 frames, played at 1 frame per second, and illustrates the changes in fluorescence detected across a septin ring as the LC polarizer progresses through the different angles of the acquisition series. The polarizer angle for each frame is given on the left. The video can be quickly imported into ImageJ for easier viewing and user control. Each panel of the video consists of contrast enhanced images of septin rings in *A. gossypii* expressing Cdc12-conGFP4 from Figs. 1–4. Top left, a whole septin ring; top middle, a partially split septin ring; top right, split septin ring; bottom left, septin accumulation at the growing hyphal tip; bottom middle, a septin ring viewed in cross section (xz perspective); bottom right, septin bars of a septin ring at a branch point.

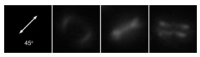

Video 2. **Polarized fluorescence acquisition of *S. cerevisiae* septin rings.** The "video" consists of 4 frames, played at 1 fps, which illustrates the changes in fluorescence detected across a septin ring as the LC polarizer progresses through the different angles of the acquisition series. The polarizer angle for each frame is given on the left. The video can be quickly imported into ImageJ for easier viewing and user control. Contrast enhanced images of septin rings in *S. cerevisiae* (Y016) expressing Cdc12-conGFP4 from Fig. 4. Left, a septin ring viewed in cross section (xz perspective); middle, a whole septin hourglass; right, a split septin ring.

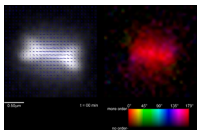

Video 3. **A loss of anisotropy occurs during septin ring reorganization.** Budding yeast (Y016) expressing Cdc12-conGFP 4 from a plasmid were grown overnight in liquid culture, transferred to a media supplemented agarose pad, covered with a coverslip, and sealed with VALAP. Polarized fluorescence images were taken every minute, through the septin ring transition. The mean dipole orientations and polarization ratios across the image were calculated and have been expressed in this video in one of two ways. (left) The mean dipole orientation is expressed as the orientation of the representative blue lines overlayed onto the fluorescence image. The length of the lines is proportional to the relative polarization ratio across the image. (right) The mean dipole orientation is expressed using the "spectrum" color scheme. The brightness of the color denotes the amount of ordered protein in the region, expressing the product of the polarization ratio and the fluorescence across the image. Each frame is 1 min apart in real time and played back at 3 frames per second. Bar, 0.5 µm.

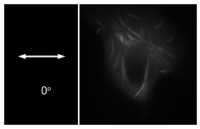

Video 4. **Polarized fluorescence acquisition of MDCK cell septin fibers.** Contrast-enhanced images of septin fibers in the MDCK cell expressing SEPT2–conGFP-1-344 from Fig. 5. The "video" consists of 4 frames, played at 1 frame per second, which illustrates the changes in fluorescence detected across the cell's septin fibers as the LC polarizer progresses through the acquisition series. The polarizer angle for each frame is given on the left. The video can be quickly imported into ImageJ for easier viewing and user control.

Table S1. **Septin filament periodicities and widths**

| Study | Figure | Periodicity | Width |
|---|---|---|---|
| | | *nm* | *nm* |
| Bertin et al., 2008 | 4 B | n/a | 11.4 ± 1.5 (n=9) |
| Bertin et al., 2008 | 4 D | 33.9 ± 3.2 (n = 5) | 12.8 ± 1.1 (n=15) |
| Byers and Goetsch, 1976 | 1 A | 30.5 ± 2.8 (n = 6) | n/a |
| Byers and Goetsch, 1976 | 1 B | 30.0 ± 2.3 (n =12) | 11.7 ± 0.9 (n=6) |
| Frazier et al., 1998 | 2 F | 33.5 ± 2.0 (n = 42) | n/a |
| Bertin et al., 2010 | 5 B | 33.6 ± 3.1 (n = 30) | n/a |
| This study | 3 B, S5 C, and unpublished data | 33.7 ± 2.6 (n = 224) | 11.4 ± 1.1 (n=176) |

Dimensions were measured based on the scale bar provided in the case of published work. n/a, not applicable, either because septins were bundled or the resolution of the image was not sufficient to make a measurement.

Table S2. **Cell strains used in this study**

| Strain | Cell type | Relevant genotype | Source |
|---|---|---|---|
| wt | *A. gossypii* | *leu2Δthr4Δ* | Altmann-Johl and Philippsen, 1996 |
| 127 | *A. gossypii* | *SHS1-GFP-NAT1*, *leu2Δthr4Δ* | Helfer and Gladfelter, 2006 |
| 296 | *A. gossypii* | *SHS1-6HA-GEN*, *leu2Δthr4Δ* | This study |
| 360 | *A. gossypii* | pAGB204 [pAg*CDC3-conGFP-GEN3 17D4*], *leu2Δthr4Δ* | This study |
| 363 | *A. gossypii* | pAGB206 [pAg*CDC12-conGFP-GEN3 0D4*], *leu2Δthr4Δ* | This study |
| 408 | *A. gossypii* | pAGB228 [pAg*CDC12-conGFP-GEN3 3D4*], *leu2Δthr4Δ* | This study |
| 409 | *A. gossypii* | pAGB229 [pAg*CDC12-conGFP-GEN 4D4*], *leu2Δthr4Δ* | This study |
| DHD5 | *S. cerevisiae* | *MATa/MATα ura3-52/ura3-52 leu2-3,112/leu2-3, 112 his3-11, 15/his3-11,15* | Schmitz et al., 2006 |
| Y010 | *S. cerevisiae* | DHD5+pAGB204[p*CDC3-conGFP-GEN 17D3*] | This study |
| Y012 | *S. cerevisiae* | DHD5+ pAGB206 [pAg*CDC12-conGFP-GEN 0D4*] | This study |
| Y015 | *S. cerevisiae* | DHD5+ pAGB228 [pAg*CDC12-conGFP-GEN 3D4*] | This study |
| Y016 | *S. cerevisiae* | DHD5+ pAGB229 [pAg*CDC12-conGFP-GEN 4D4*] | This study |
| S2 | MDCK | pS2 [p*EGFP-SEPT2*] | This study |
| S2 1-344 | MDCK | pS2-1 [$SEPT2_{1-7}$-$EGFP_4$] | This study |
| S2 1-340 | MDCK | pS2-2 [$SEPT2_{1-21}$-$EGFP_4$] | This study |

Except for Nos. 127 and 296, which are an integrated homokaryons, all analyzed cells were expressing septin constructs from a plasmid. Genotypes are listed in brackets.

Table S3. **Plasmids used in this study**

| Plasmid No. | Name | Vector | Relevant insert | Source |
|---|---|---|---|---|
| AGB005 | pAGT 141 | pUC19 | *GFP-GEN3* | Kaufmann, 2009 |
| AGB123 | pAG CDC12 | pRS416 | *CDC12* | DeMay et al., 2009 |
| AGB127 | pAG CDC3 | pRS416 | *CDC3* | Dietrich et al., 2004 |
| AGB 204 | Cdc3-conGFP-GEN (17D4) | pRS416 | *CDC3-conGFP-GEN3 (17D4)* | This study |
| AGB 206 | Cdc12-conGFP-GEN (0D4) | pRS416 | *CDC12-conGFP-GEN 3(0D4)* | This study |
| AGB228 | Cdc12-conGFP-GEN (3D4) | pRS416 | *CDC12-conGFP-GEN 3(3D4)* | This study |
| AGB229 | Cdc12-conGFP-GEN (4D4) | pRS416 | *CDC12-conGFP-GEN 3(4D4)* | This study |
| AGB35 | pAGT125 | pUC19 | 6HA-*GEN3* | Kaufmann, 2009 |
| pEGFP | pEGFP-N1 | | EGFP | Takara Bio, Inc. |
| pS2 | EGFP-SEPT2 | | *EGFP-SEPT2* | This study |
| pS2-17 | SEPT2-EGFP 1-344 | | *SEPT2-EGFP 1-344* | This study |
| pS2-21 | SEPT2-EGFP 1-340 | | *SEPT2-EGFP 1-340* | This study |

Table S4. **Oligonucleotide primers used in this study**

| Primer No. | Name | Sequence |
|---|---|---|
| AGO37 | VG3 | 5′-ATGTTGGACGAGTCGGAATC-3′ |
| AGO36 | VG5 | 5′-GGAGGTAGTTTGCTGATTGG-3′ |
| AGO197 | 5′ Cdc12 25ds F2a | 5′-GTAGTATCGCTGTATATCTTCAACATTGCGATCTGCTGTAAACCACTGCAGGCATGCAAGCTTAG-3′ |
| AGO313 | 6HA G3 R | 5′-CTAGTAGCAAACGTGTCCTCAGTTCCCGCGTTCTGTTACATACCCCTGCAGGCATGCAAGCTTAG-3′ |
| AGO324 | SHS1 6HA F seq | 5′-GTGATGGATATGCTTCCCGC-3′ |
| AGO325 | SHS1 6HA R seq | 5′-CCGCGTTCTGTTACATACCC-3′ |
| AGO328 | SHS1-6HA F | 5′-GCTAGTGATGGATATGCTTCCCGCGCAACAGGCCAGGTACAAACGACGGCCAGTGAATTCGAG-3′ |
| AGO365 | 5′ Sep7 tag | 5′-CTCCATCTGCCGACTCTAGTC-3′ |
| AGO403 | Tef2T R | 5′-GTGCCGAGTTGGAGGACATC-3′ |
| AGO504 | Cdc3 17D3GFP:GEN F | 5′-CAACTCAAAGCTTTGGAGGAGAAAAAGCACCAGTTGGAGATGTCTTTGGCGGAAGAACTTTTCACTGGA GTTG-3′ |
| AGO505 | Cdc3 constrained GFP R | 5′-GGGTAACAGGGGAGGGAAATAAAATGCATGCATAGAAGTAAAGTGCATGATTACGCCAAGCTTGC-3′ |
| AGO525 | Cdc12 0D4 GFP F | 5′-AAGGTTAAGAAGCTGGAGGAGCAGGTCAGAGCATTGCAACTAAGAAAGCACGAAGAACTTTTCACTGG AGTTG-3′ |
| AGO608 | Cdc12 3D4 GFP F | 5′-CAGGCCAAGGTTAAGAAGCTGGAGGAGCAGGTCAGAGCATTGCAACTAGAAGAACTTTTCACTGGAG-TTG-3′ |
| AGO609 | Cdc12 4D4 GFP F | 5′-CAGGCCAAGGTTAAGAAGCTGGAGGAGCAGGTCAGAGCATTGCAAGAAGAACTTTTCACTGGAGTTG-3′ |
| | S2-F | 5′-CCGCTCGAGCCACCATGTCTAAGCAACAACC-3′ |
| | S2-R | 5′-CGGGATCCCGCACATGCTGCCCGAGAG-3′ |
| | S2-C-seq | 5′-GATGAAATTGAAGAGC-3′ |
| | S2-21-F | 5′-GCAAGAGATGATTGCAAGAATGCAAGGCGAGGAGCTGTTCACC-3′ |
| | S2-21-R | 5′-GGTGAACAGCTCCTCGCCTTGCATTCTTGCAATCATCTCTTGC-3′ |
| | S2-17-F | 5′-GCAAGAATGCAAGCGCAGATGCAGGGCGAGGAGCTGTTCACC-3′ |
| | S2-17-R | 5′-GGTGAACAGCTCCTCGCCCTGCATCTGCGCTTGCATTCTTGC-3′ |

## References


Altmann-Jöhl, R., and P. Philippsen. 1996. AgTHR4, a new selection marker for transformation of the filamentous fungus Ashbya gossypii, maps in a four-gene cluster that is conserved between *A. gossypii* and *Saccharomyces cerevisiae. Mol. Gen. Genet.* 250:69–80.

Bertin, A., M.A. McMurray, P. Grob, S.S. Park, G. Garcia III, I. Patanwala, H.L. Ng, T. Alber, J. Thorner, and E. Nogales. 2008. *Saccharomyces cerevisiae* septins: supramolecular organization of heterooligomers and the mechanism of filament assembly. *Proc. Natl. Acad. Sci. USA*. 105:8274–8279. doi:10.1073/pnas.0803330105

Bertin, A., M.A. McMurray, L. Thai, G. Garcia III, V. Votin, P. Grob, T. Allyn, J. Thorner, and E. Nogales. 2010. Phosphatidylinositol-4,5-bisphosphate promotes budding yeast septin filament assembly and organization. *J. Mol. Biol.* 404:711–731. doi:10.1016/j.jmb.2010.10.002

Byers, B., and L. Goetsch. 1976. A highly ordered ring of membrane-associated filaments in budding yeast. *J. Cell Biol.* 69:717–721. doi:10.1083/jcb.69.3.717

DeMay, B.S., R.A. Meseroll, P. Occhipinti, and A.S. Gladfelter. 2009. Regulation of distinct septin rings in a single cell by Elm1p and Gin4p kinases. *Mol. Biol. Cell*. 20:2311–2326. doi:10.1091/mbc.E08-12-1169

Dietrich, F.S., S. Voegeli, S. Brachat, A. Lerch, K. Gates, S. Steiner, C. Mohr, R. Pöhlmann, P. Luedi, S. Choi, et al. 2004. The *Ashbya gossypii* genome as a tool for mapping the ancient *Saccharomyces cerevisiae* genome. *Science*. 304:304–307. doi:10.1126/science.1095781

Frazier, J.A., M.L. Wong, M.S. Longtine, J.R. Pringle, M. Mann, T.J. Mitchison, and C. Field. 1998. Polymerization of purified yeast septins: evidence that organized filament arrays may not be required for septin function. *J. Cell Biol.* 143:737–749. doi:10.1083/jcb.143.3.737

Helfer, H., and A.S. Gladfelter. 2006. AgSwe1p regulates mitosis in response to morphogenesis and nutrients in multinucleated *Ashbya gossypii* cells. *Mol. Biol. Cell*. 17:4494–4512. doi:10.1091/mbc.E06-03-0215

Kaufmann, A. 2009. A plasmid collection for PCR-based gene targeting in the filamentous ascomycete *Ashbya gossypii. Fungal Genet. Biol.* 46:595–603. doi:10.1016/j.fgb.2009.05.002

Schmitz, H.P., A. Kaufmann, M. Köhli, P.P. Laissue, and P. Philippsen. 2006. From function to shape: a novel role of a formin in morphogenesis of the fungus *Ashbya gossypii. Mol. Biol. Cell*. 17:130–145. doi:10.1091/mbc.E05-06-0479